
Supplementary Information (SI)

for

Double metal-free polymer reactive sites for the efficient degradation of diclofenac by visible light-driven oxygen reduction to superoxide radical and hydrogen peroxide

Qianxin Zhang^a, Cuiwen Tan^a, Xiaoshan Zheng^a, Ping Chen^{a,b}, Meihui Zhuo^a, Tiansheng Chen^a, Zhijie Xie^a, Fengliang Wang^a, Haijin Liu^c, Xiangdan Zhang^a, Yang Liu^d, Wenyng Lv^{a*}, Guoguang Liu^{a*}

^a*School of Environmental Science and Engineering, Guangdong University of Technology, Guangzhou, 510006, China*

^b*School of Environment, Tsinghua University, Beijing, 100084, China*

^c*Key Laboratory for Yellow River and Huaihe River Water Environment and Pollution Control, School of Environment, Henan Normal University, Xinxiang 453007, China*

^d*Faculty of Environmental and Biological Engineering, Guangdong University of Petrochemical Technology, Maoming 525000, China*

*** Corresponding Author:** Wenyng Lv, E-mail: lvwy612@163.com, Telephone: +86-20-39322547, Fax: +86-13538982812

Guoguang Liu, E-mail: liugg615@163.com, Telephone: +86-20-39322547, Fax: +86-20-39322548;

Summary:

Number of pages: 20

Number of tables: 3

Number of figures: 13

Text

Text S1. Photoanode preparation: Indium tin oxide (ITO) glass was initially obtained through sequential rinsing with acetone, distilled water, and ethanol in an ultrasonic cleaner for 30 min. Subsequently, 1.0 mg of the photocatalyst was well dispersed in 0.5 ml ethanol with 10 μ l Nafion under ultrasonic treatment for 30 min. Afterward, the above suspension was deposited dropwise onto an ITO glass surface with uniformly exposed area of $1 \times 1 \text{ cm}^2$. Following drying overnight in an oven, the electrodes were sintered at 60°C in N₂ for 2 h to improve adhesion.

Text S2. Determination of concentration of PPCPs. The concentration of PPCPs was analyzed via Waters alliance e2695-2998 high performance liquid chromatography (HPLC, USA), which was equipped with a C18 reversed-phase column (XBridge, 4.6 \times 250 mm, 5 μm).

Text S3. Intermediates Identification by HRLC-MS-MS. The photocatalytic degradation intermediates of DCF were identified by HRLC-MS-MS (Thermo Scientific Ultimate 3000 RSLC and Q Exactive Orbitrap). Separation was accomplished using an Hypersil GOLD C18 (100 \times 2.1 mm, 1.9 μm) with column temperature 40 °C. Elution was performed at a flow rate of 0.3 mL/min with water that contained 0.1 % (v/v) formic acid as eluent A, and methanol as eluent B. Mass spectral analysis was conducted in negative mode.

Tab. S1 Mobile phase composition and gradient elution table

Time (min)	%A	%B
0	98	2
2	98	2
16	5	95
18	5	95
18.1	98	2
20	98	2

Tab. S2 Mass spectrum scanning parameters

parameters	value
Sheath gas flow rate	40
Aux gas flow rate	10
Sweep gas flow rate	0
Spray voltage (l KV)	+3.5, -2.5
Capillary temp. (°C)	320
Aux gas heater temp. (°C)	350

Tab. S3 Mass spectrum scanning parameters

Mass spectrum scanning parameters	value
Scan mode	+, - Full MS-ddMS2
Full MS scan range	150-1000 m/z
Resolution	Full MS: 70,000 FWHM MS/MS: 17,500 FWHM
Isolation width	1.0 m/z
NCE (Stepped NCE)	40 (50%)

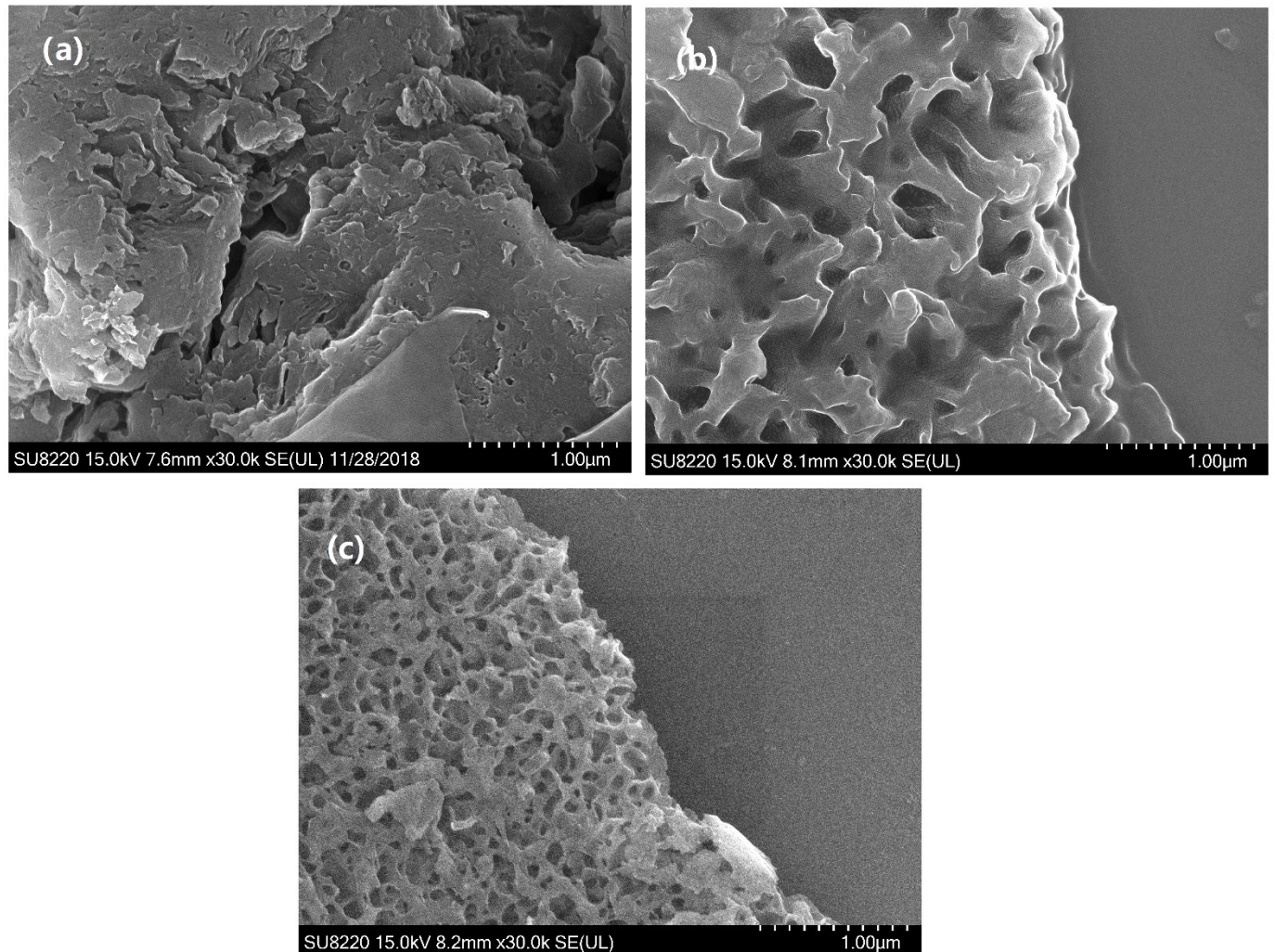


Fig.SI SEM of $g\text{-}C_3N_4$ and OCN and CDs/OCN

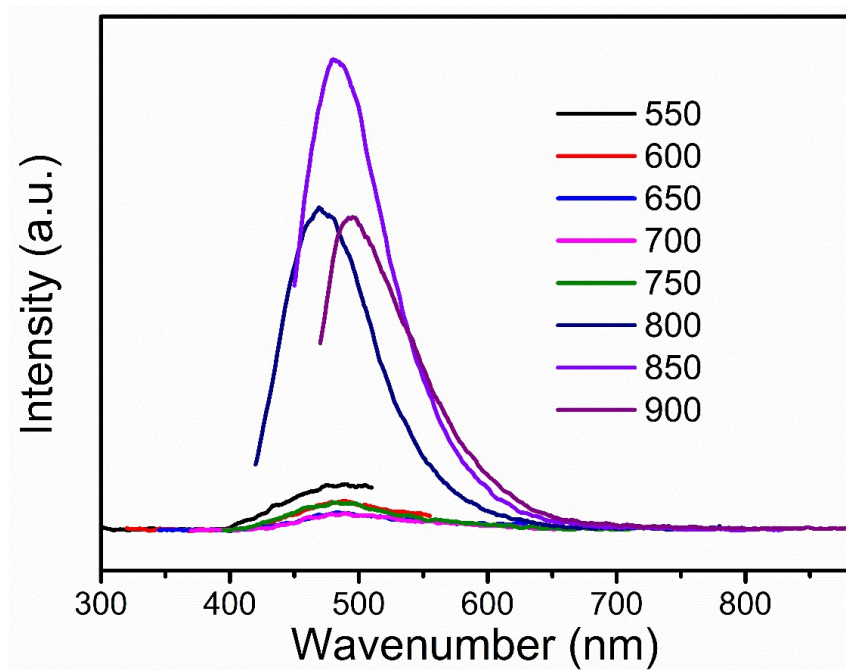


Fig. S2 The Up-conversion fluorescence spectrum of CDs

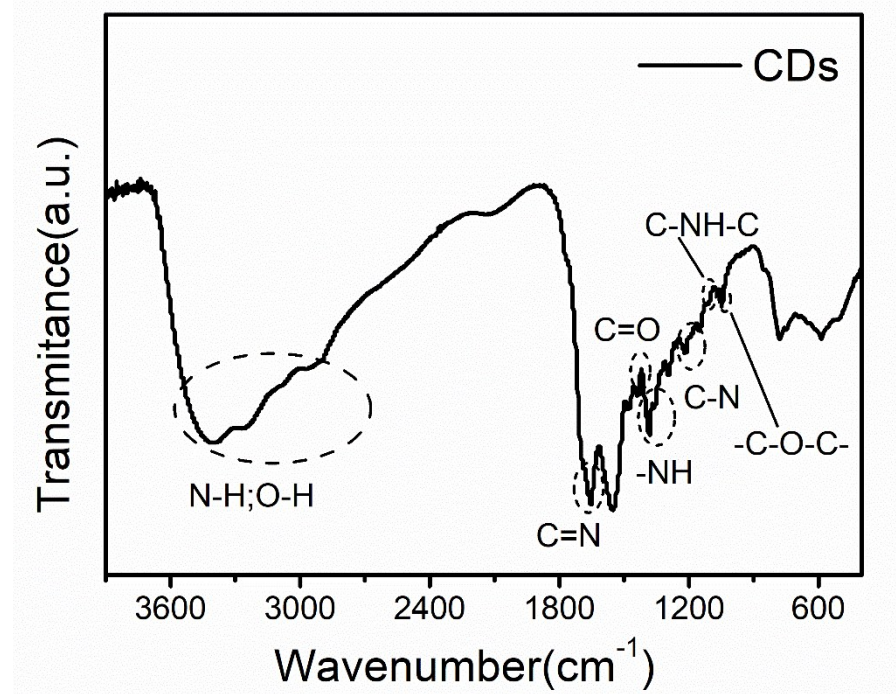


Fig. S3 The FTIR spectrum of CDs

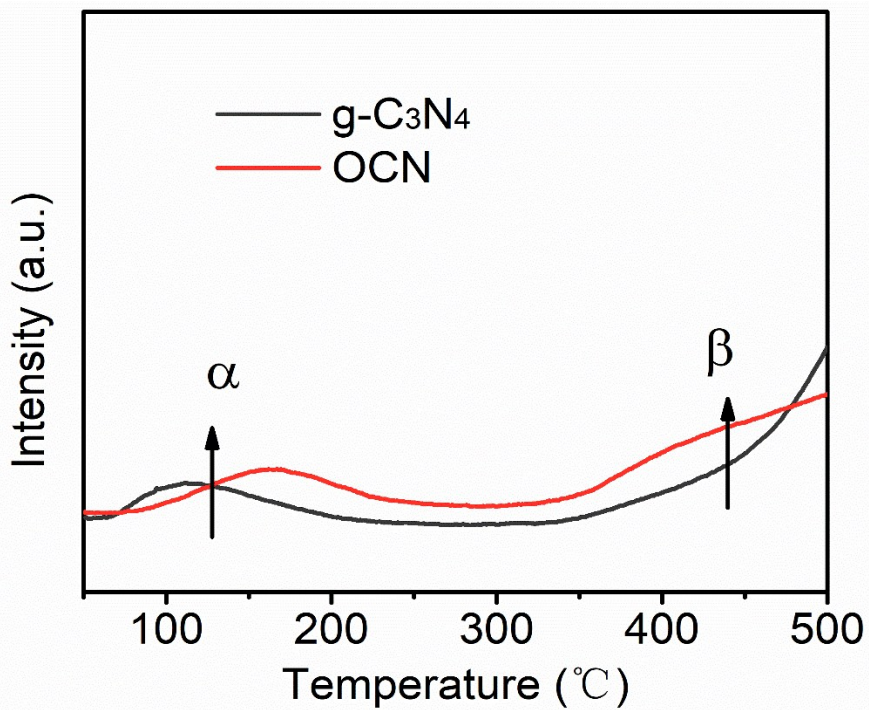
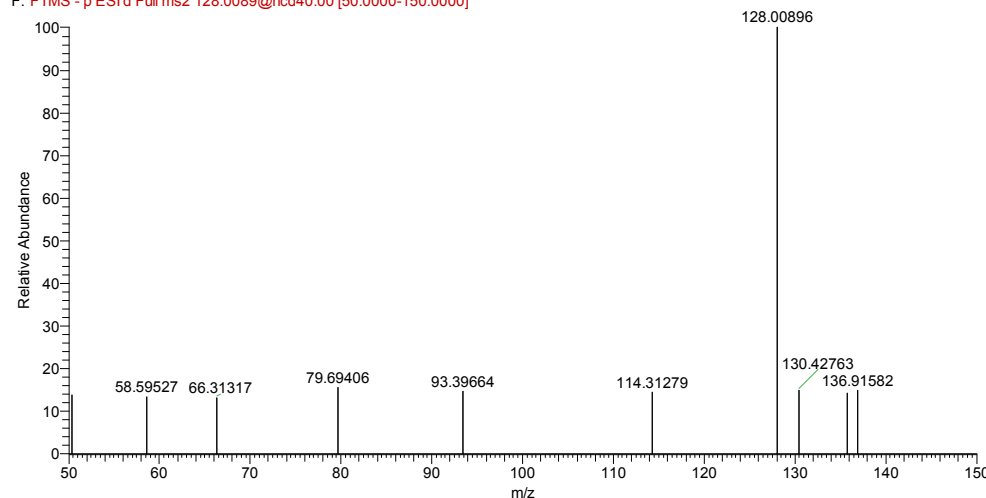
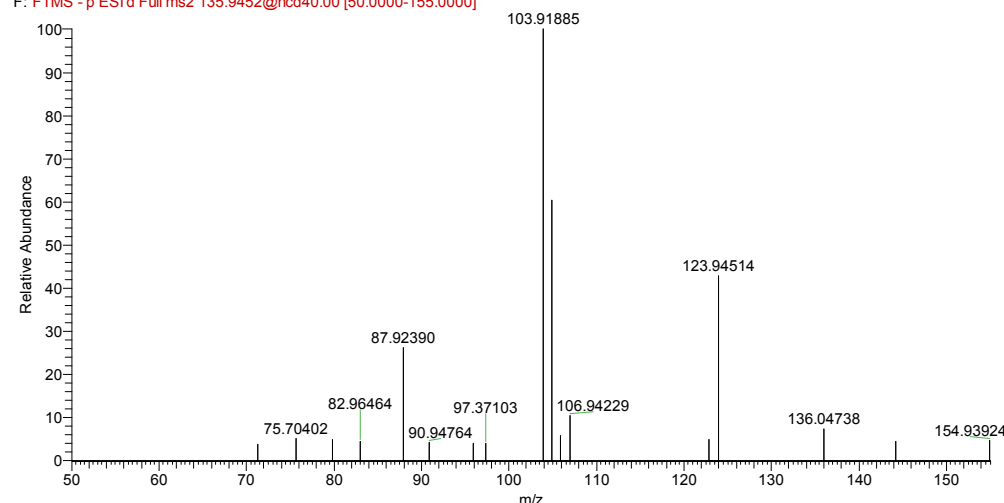


Fig.S4 O₂-TPD of g-C₃N₄ and OCN

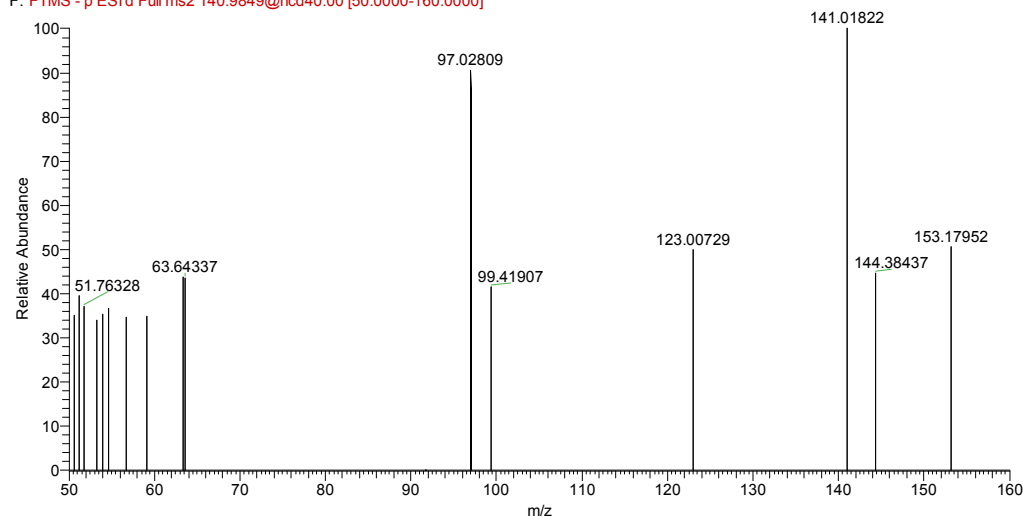
DCF #369 RT: 1.05 AV: 1 NL: 1.35E4
F: FTMS - p ESId Full ms2 128.0089@hcd40.00 [50.0000-150.0000]

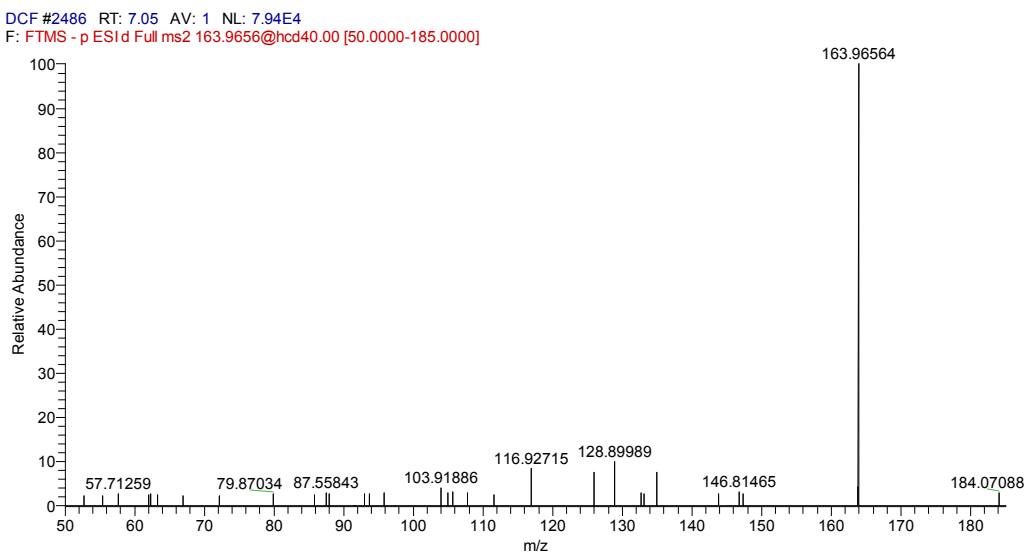
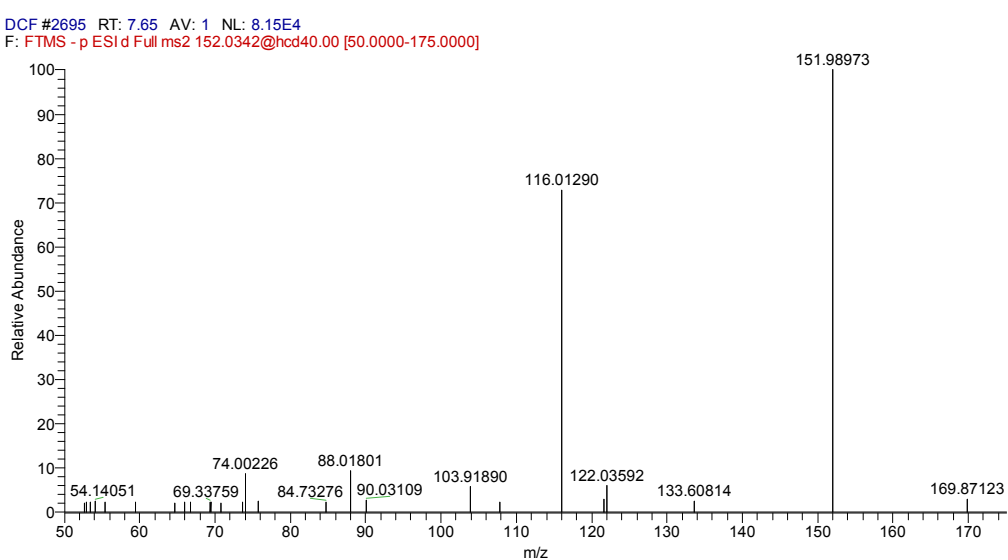
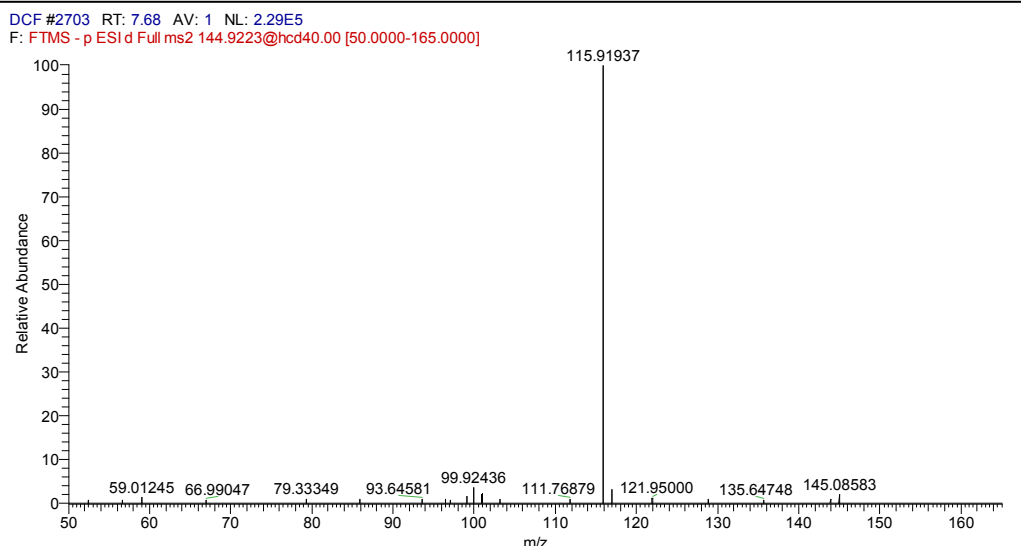


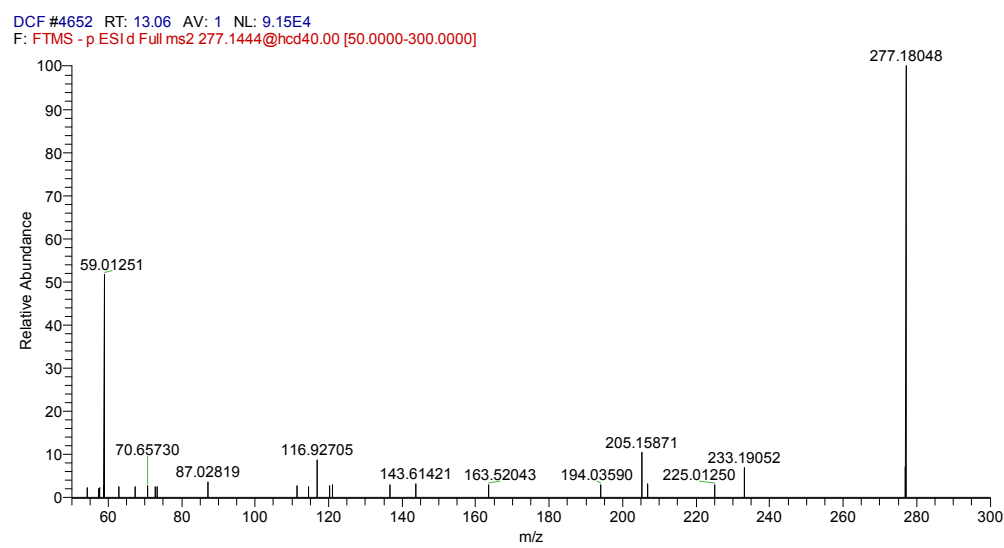
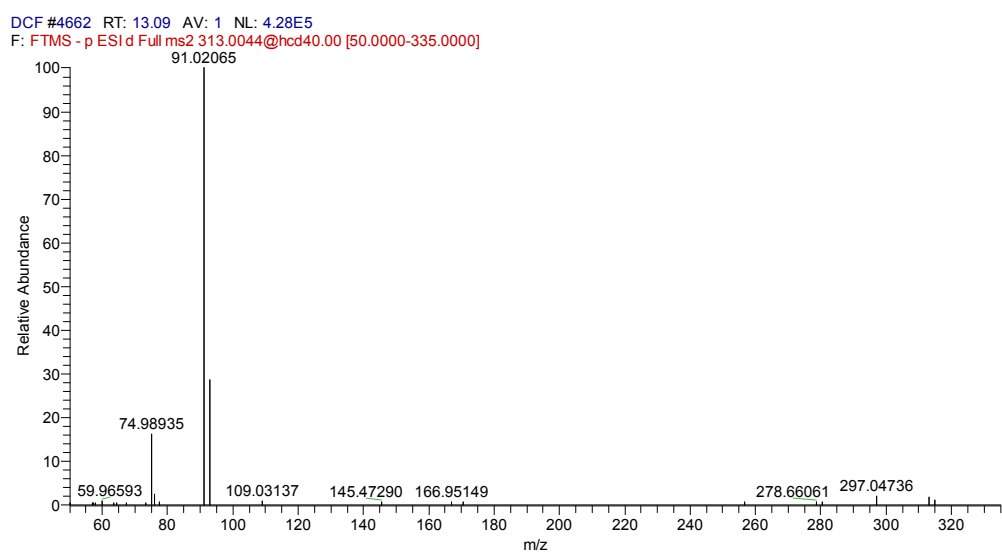
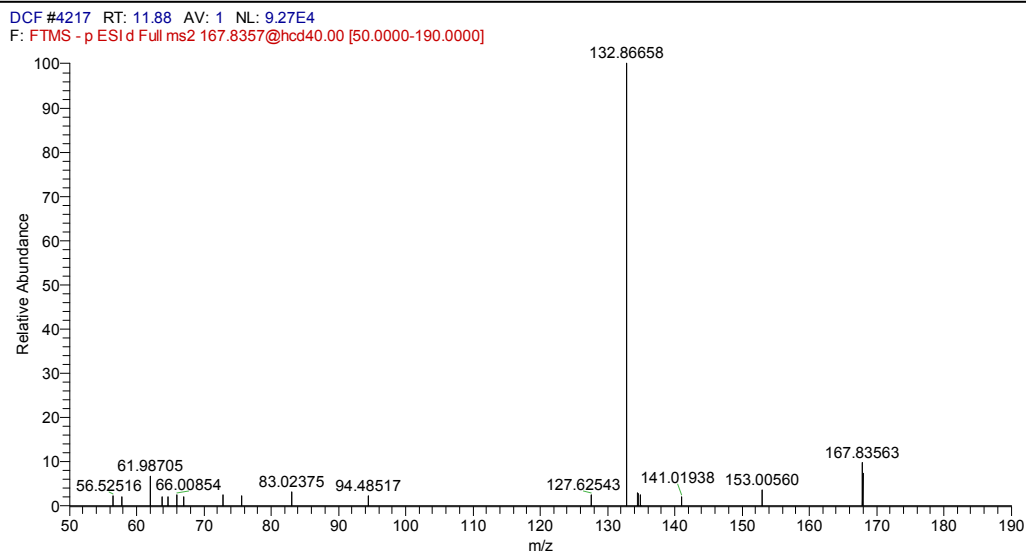
DCF #277 RT: 0.79 AV: 1 NL: 4.58E4
F: FTMS - p ESId Full ms2 135.9452@hcd40.00 [50.0000-155.0000]



DCF #314 RT: 0.89 AV: 1 NL: 4.73E3
F: FTMS - p ESId Full ms2 140.9849@hcd40.00 [50.0000-160.0000]







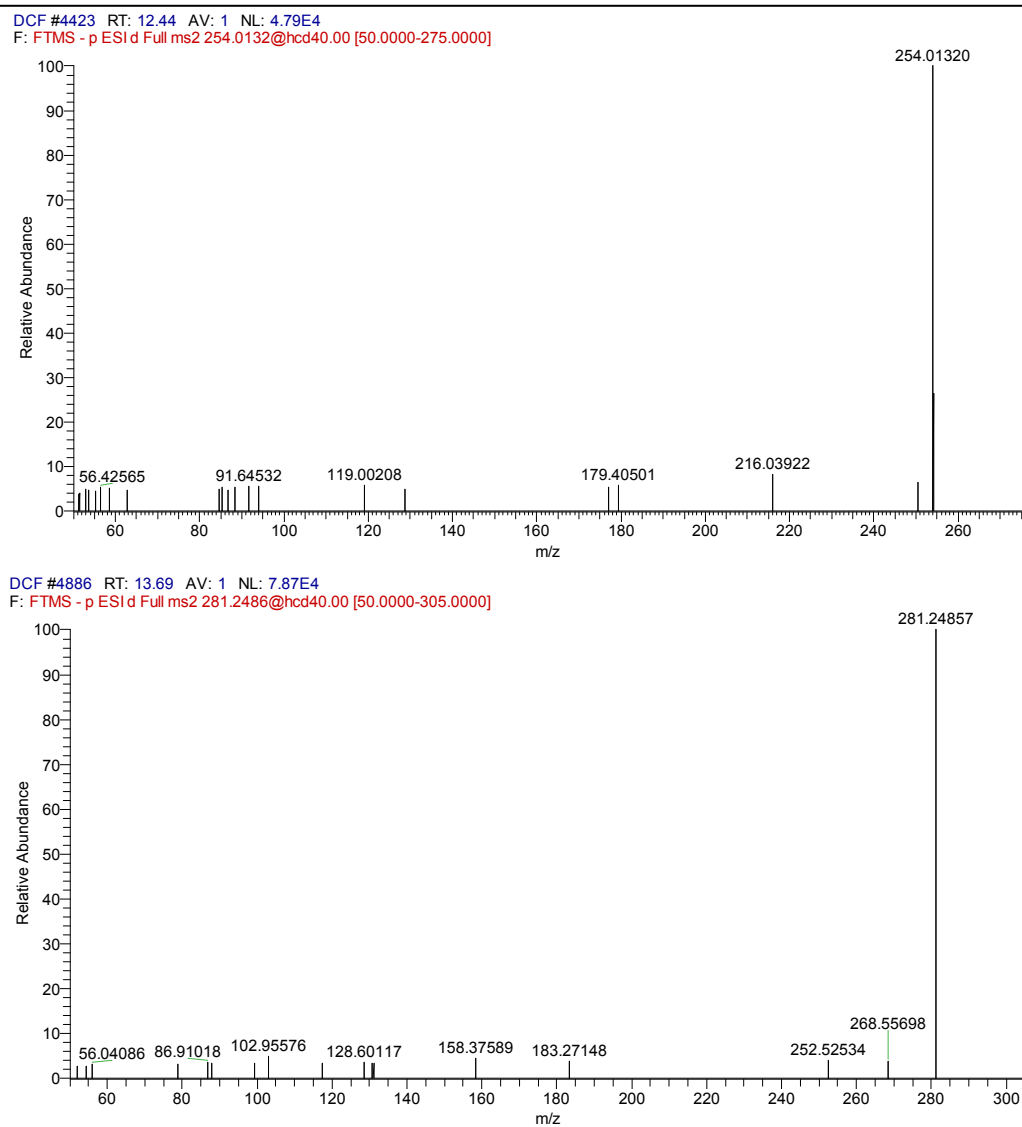


Fig. S5 MS/MS fragmentation analyses of the observed transformation products of DCF.

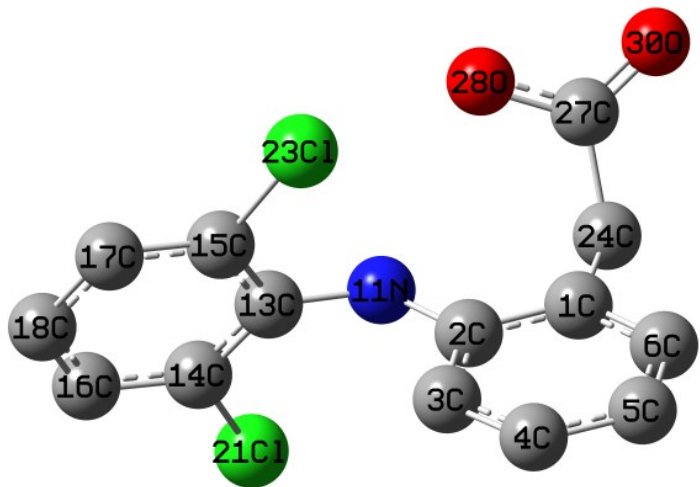


Fig. S6. The atomic model of DCF

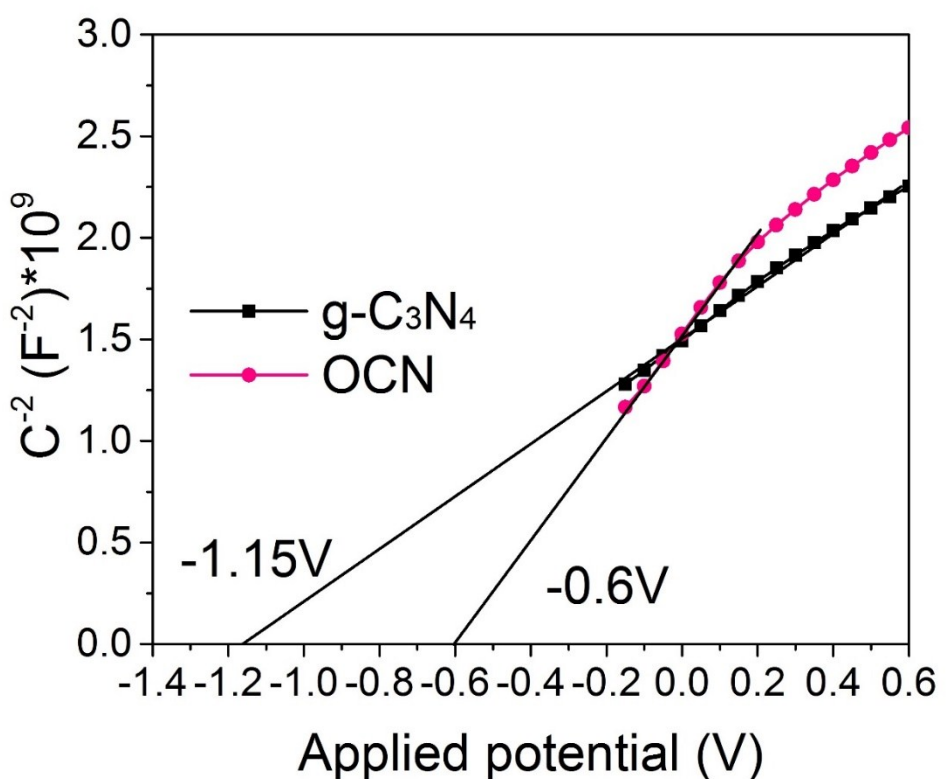


Fig. S7. The Mott–Schottky plots of the catalysts¹

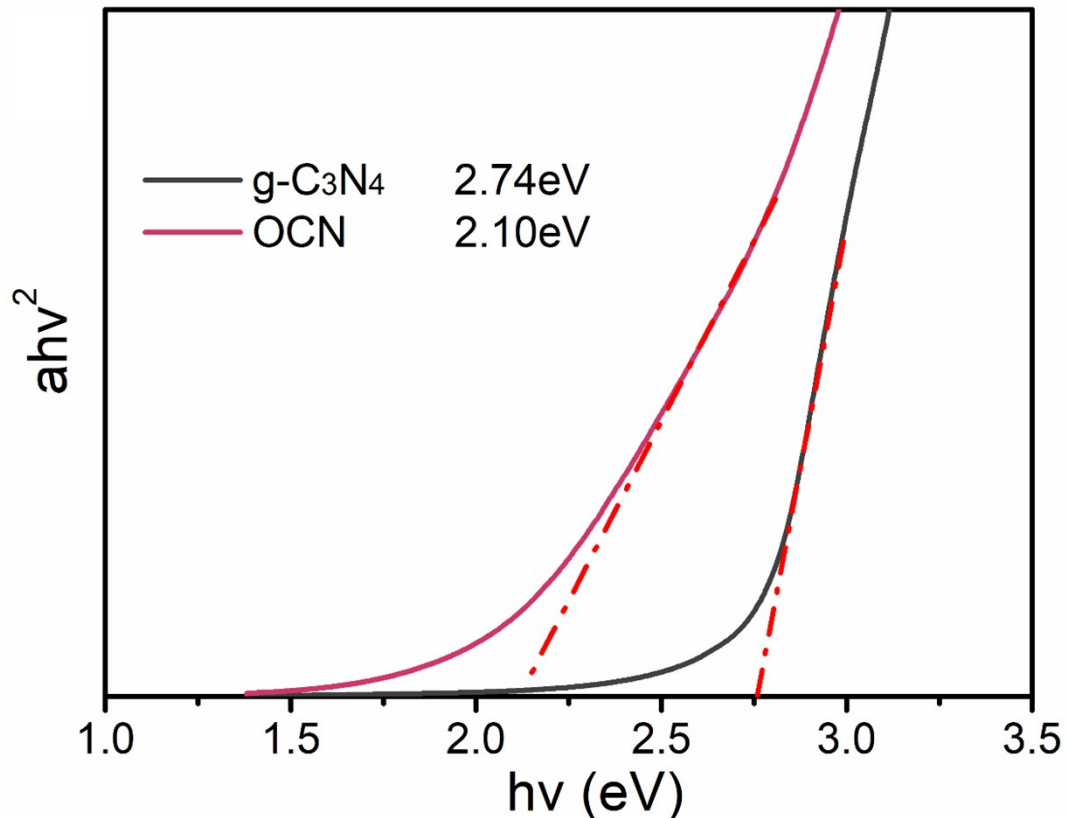


Fig.S8. The Kubelka–Munk formula of the as-samples

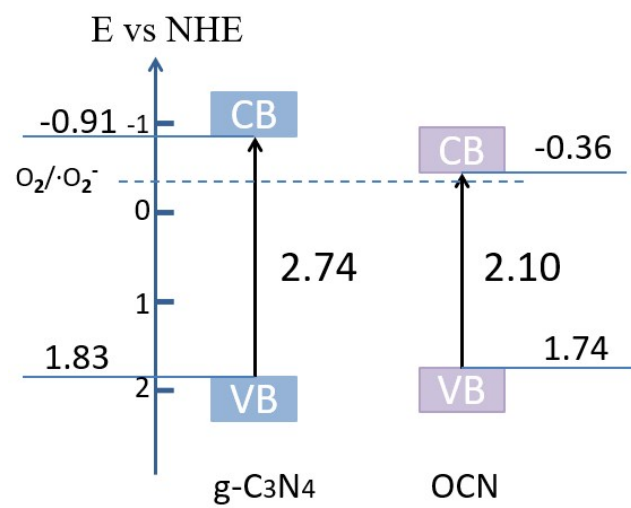


Fig. S9. Band structure alignments of $g\text{-C}_3\text{N}_4$ and OCN

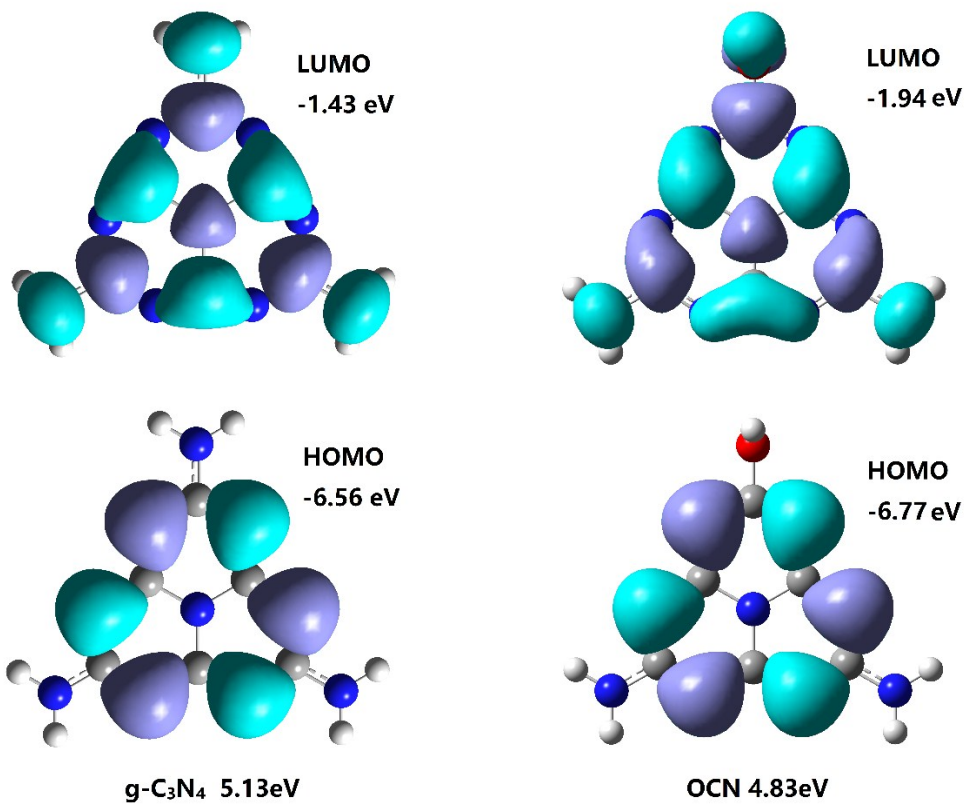


Fig. S10. Interfacial plots of main orbitals for (a) $g\text{-C}_3\text{N}_4$, (b) OCN models, calculated at the DFT level (B3LYP/6- 311G (d, p)).

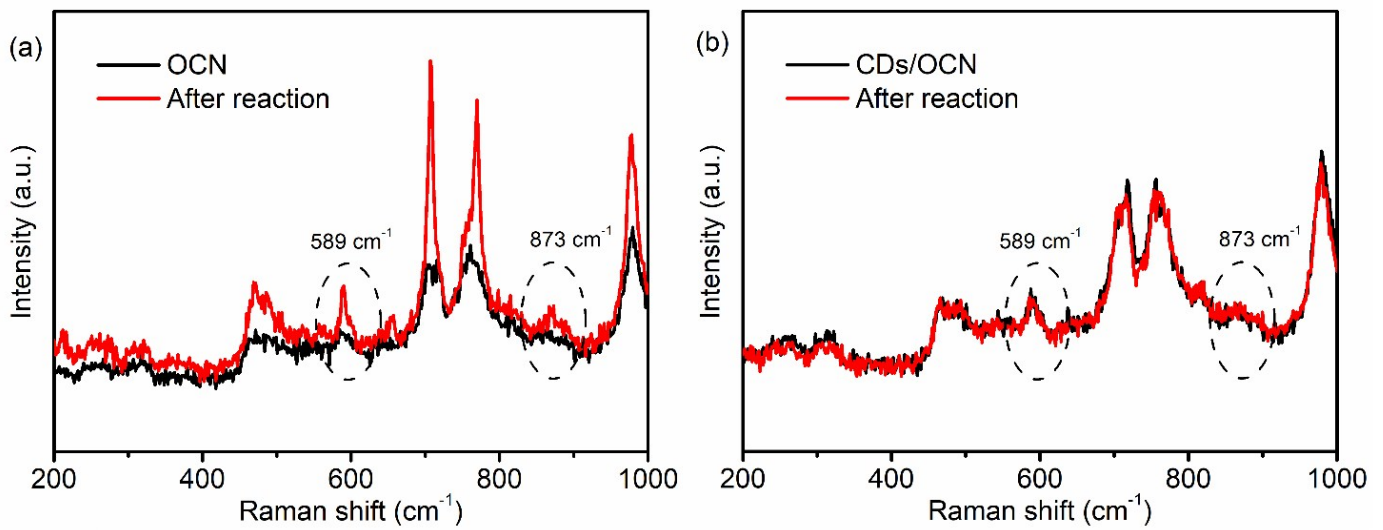


Fig. S11. The Raman spectra of the OCN(a) and CDs/OCN(b) before and after the reaction

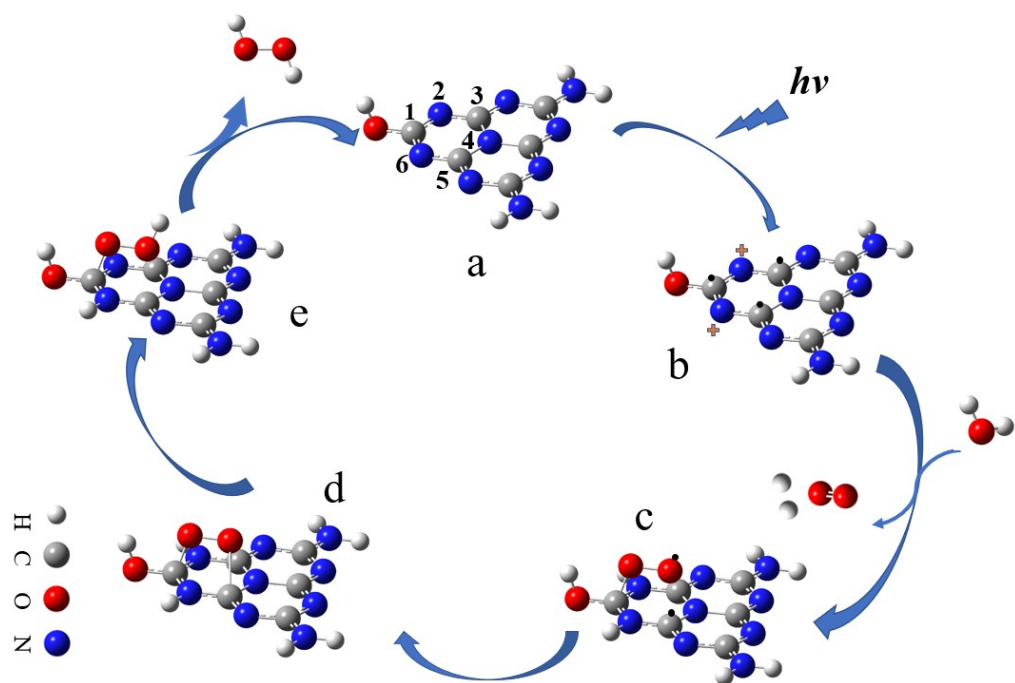


Fig.S12 The mechanism of OCN facilitated photocatalytic O_2 reduction to synthesize H_2O_2 .

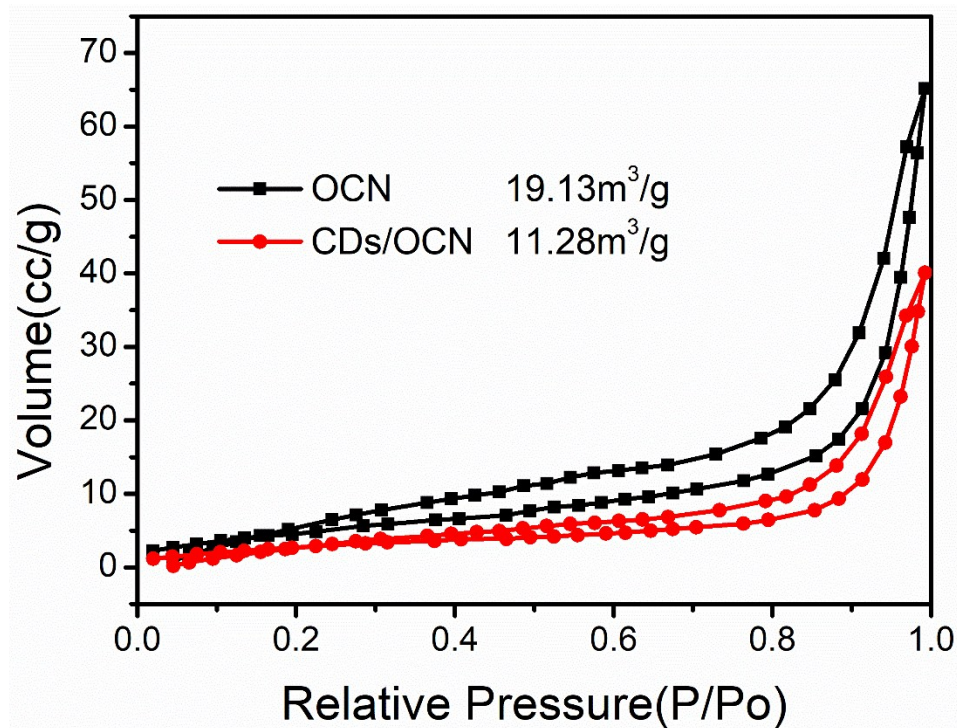


Fig. S13. The N_2 adsorption–desorption isotherms

Reference

1. Q. X. Zhang, P. Chen, C. W. Tan, T. S. Chen, M. H. Zhuo, Z. J. Xie, F. L. Wang, H. J. Liu, Z. W. Cai, G. G. Liu and W. Y. Lv, A photocatalytic degradation strategy of PPCPs by a heptazine-based CN organic polymer (OCN) under visible light, *Environ Sci-Nano*, 2018, **5**, 2325-2336.